Tuijin Jishu/Journal of Propulsion Technology
ISSN: 1001-4055
Vol. 44 No. 6 (2023)

Study of Friction Behavior in Aluminum-Based Composites Reinforced with B_4C, SiC, and Al_2O_3 Particles

Yashar Vatandoust[1], Mohammad Zadshakoyan[2]
[1,2]*Department of Manufacturing and Production Engineering, Faculty of Mechanical Engineering, University of Tabriz, Tabriz, Iran*

Abstract:- In this research, five types of aluminum-based composites with 20% reinforcing particles of B_4C, SiC, and Al_2O_3, as well as dual-phase combinations of SiC/B_4C and B_4C / Al_2O_3, were fabricated using the powder metallurgy method. A single-stage hot extrusion process was performed on these composites. Friction tests were conducted on each of these specimens, and the results, including wear rate and coefficient of friction, were graphically represented. These results were compared with the properties of pure aluminum. Additionally, some of the extrusion and compression parameters were investigated. The obtained results indicate that by adding ceramic particles, the wear rate is significantly reduced compared to pure aluminum made by the same method. Furthermore, the coefficient of friction of the specimens is lower compared to pure aluminum. Among the ceramic reinforcement particles, two types of composites, Al-20% SiC and Al-20% B_4C, showed better results than the other composites. In most tests, they exhibited the lowest values in terms of wear rate and coefficient of friction. The increase or decrease in the coefficient of friction and wear rate is subject to an extreme condition with respect to vertical force or sliding velocity, the values of which depend on the friction test parameters.

Keywords: Metal Matrix Composite, Wear Rate, Ceramic Particles, Powder Metallurgy

Introduction

The phenomenon of metal wear in industries producing automotive brakes or trains has always been a subject of interest for researchers and industry professionals. The study of wear rates and friction coefficients, taking into consideration the heat generated due to friction, has been a recurrent topic of research for various materials, including both metallic and composite materials. Numerous experiments have been conducted to investigate the wear rate and friction coefficient of metal matrix composites (MMCs), particularly aluminum-based composites with varying volume fractions of reinforcing particles such as Al_2O_3, SiC, and B_4C. These investigations have been carried out under both constant and variable pressure forces and sliding velocities, and their results have found applications in various aerospace industries.

In the case of wear rate and friction coefficient for Al-SiC and Al-B_4C composites under variable sliding velocity and constant pressure force conditions, friction tests were conducted using a pin-on-disc composite method at two different sliding speeds, 4.17 and 1.62 *m/s*, and a constant pressure of 0.75 MPa. The results showed that at higher sliding velocities, the wear rate and coefficient of friction decreased for both types of composites. Specifically, as the sliding speed increased from 1.62 to 4.17 m/s, the wear rate for both types of composites decreased from 3.5 * 10^{-7} to 1.5 * 10^{-7} grams per meter, and the coefficient of friction decreased from 4.5 to 3.5 for each meter traveled [1].

The authors of this article conducted wear tests on Al-13%SiC and Al-13%B_4C composites under constant speed conditions (1.62 *m/s*) and varying pressure (0.75-3.00 *MPa*). They found that the wear rate and surface roughness increased with increasing pressure. Specifically, with an increase in pressure from 0 to 3.0 MPa, the wear rate increased between 0-6 (mm^3/m) * 10^{-4} [2].

The friction behavior and wear rate of the composite disc were also tested under both variable speed and variable force conditions. The results indicated that the wear rate decreased with an increase in force between 30-40 *N* and increased between 1-3 (mm^3/m) * 10^{-4} with an increase in force from 50-100 *N*. Additionally, the wear rate of the composite decreased with increasing speed. The wear rate of the composite was higher than that of cast iron between speeds of 3-9 *m/s* under a force of 30 *N*, and there was not much difference between them under a force of 50 *N*. However, under a force of 100 *N*, the wear rate of the composite was significantly higher than that of cast iron [3].

In reference [4], the authors conducted a study on the effect of sliding velocity using a pin-on-disc method on the wear rate and subsurface deformation of two types of composites: Al 2219/15 SiCp and Al 2219/15 SiCp-3 graphite. They concluded that adding reinforcing particles to pure aluminum improves its wear resistance. However, adding graphite particles results in an excessive increase in wear resistance.

In article [5], the authors investigated the friction behavior of Al-SiC composites with varying volume fractions of particles under different applied forces (5, 7, 9, 11 *Kgf*) and constant sliding velocity (1.0 *m/s*) using a pin-on-disc method. They found that the wear rate increases with increasing applied pressure. However, in general, the wear rate of the composites is lower compared to pure aluminum. The friction coefficient decreases with increasing pressure for both pure aluminum and composites.

In reference [6], a similar experiment to the one in article [5] was conducted with a constant force of 2 *N* using the pin-on-disc method. The results showed that the wear resistance of aluminum with reinforcing particles is greater than that of pure aluminum. This wear resistance increases with the size and quantity of the particles. In article [7], the Al-Si-SiCp composite was tested to investigate its friction and wear behavior using the pin-on-disc method. The surface finish was examined using SEM (Scanning Electron Microscopy). In article [8], two types of Al-SiC/25% composites with different particle sizes (34 μm and 3.5 μm) were subjected to tests under varying forces and velocities. Additionally, the study explored what happens to the friction coefficient at temperatures of 316°C and 177°C. In article [9], an aluminum-based composite reinforced with iron aluminide particles was studied to investigate wear rates. Finally, in article [10], a composite consisting of SiC and Al_2O_3 fibers on a 440C stainless steel disc was examined to investigate frictional and surface characteristics. In article [11], the effect of load and temperature on the frictional and wear behavior of two types of aluminum-based composites with 10% and 20% volume fractions of SiC reinforcing particles was investigated. The study also examined the wear mechanisms for loads less than 200 *N* and greater than 200 *N*.

In all of these studies, the authors have consistently observed that the wear rate of composites increases with an increase in applied force. Additionally, the wear rate decreases with an increase in sliding velocity within a specific range. An increase in applied pressure force leads to a reduction in the coefficient of friction within a certain range, and beyond that range, it increases. Furthermore, increasing sliding velocity results in a decrease in the coefficient of friction. These results are consistent across nearly all of the research conducted. The objective of this research is to determine the wear rate and coefficient of friction for composite materials with an aluminum-based matrix and ceramic reinforcing particles such as SiC, B_4C, and Al_2O_3. These composites are produced separately and in combination using the powder metallurgy process and extrusion. The study also aims to investigate the influence and role of each type of particle in the wear behavior, including wear rate and coefficient of friction, of these composites. To achieve this, the results obtained from wear tests will be initially presented in graphical form, and then the data from these graphs will be thoroughly examined. Finally, the optimal combination among the tested compositions will be discussed.

Research Methodology:

In this study, the initial materials were provided in the form of powders, encompassing four types: aluminum (Al), silicon carbide (SiC), boron carbide (B_4C), and aluminum oxide (Al_2O_3). The specifications of these powders are detailed in Table (1).

Table 1: Specifications of the powders used

Notch Hardness	Density $^{gr}/_{cm^3}$	Melting point	Sintering temperature °C	Grain size	Particle size μm	Powder type	Powder material
	2.76	660	600	P 280	52	Metallic	Al
2480	3.21	2700	1750-2100	P 800	20	Ceramic	SiC
2800	2.52	2763	2104-2220	P 280	52	Ceramic	B_4C
2000	3.92	2050	1400-1800	P 280	52	Ceramic	Al_2O_3

The samples were produced in two stages in cylindrical form. The first stage is the sample obtained from powder compaction, such that their length is less than their diameter. This is done to eject the part from the die without cracking or scratching, and also to improve the compaction density of the final part. Figure 1 shows some of the sound and defective samples from this stage.

Dimensions of cylindrical samples obtained from powder compaction ϕ36*22mm

Figure 1: Samples from stage 1, where the parts on the left are sound and the parts on the right are broken or scratched due to not following the diameter to height ratio.

The second stage involves preparing cylindrical specimens obtained from the extrusion of the samples from the first stage. These cylindrical specimens have a length significantly greater than their diameter. The dimensions of the extruded specimens are ϕ14*150mm. The extrusion process was carried out to increase the density of the components and to meet the wear characteristics requirements. An extruded specimen is depicted in Figure (2).

Figure 2: Extruded sample with some length machined to prepare for wear testing.

These specimens are composed of six different combinations of four types of powders: Al, SiC, B_4C, and Al_2O_3. Table (2) presents the types and volume percentages of the powders used to form the specimens. The weight of the powders was calculated for each specimen based on the specimen's volume, the density of the powder materials, as specified in Table (1), and the predicted volume percentage of each powder.

Table 2: Volume percentage and type of powders comprising the samples

Sample number	1	2	3	4	5	6
Combination type	100%Al	80%Al+ 20%SiC	80%Al+ 20%Al_2O_3	80%Al+ 20%B_4C	80%Al+ 20%[75%SiC+ 25%B4C]	80%Al+ 20%[75%Al2O3+ 25%B4C]

The weighing of powders was carried out using a digital scale with a precision of 0.01 grams.

Powder Compaction:

To compact the powders, we used a die with a cylindrical cavity and a unidirectional punch, as shown in Figures (3) and (4). Pressure was applied from one direction using the punch from the top to compact the powder. After compaction and removal of the bottom punch, the upper punch continued to move to eject the compacted component from within the die.

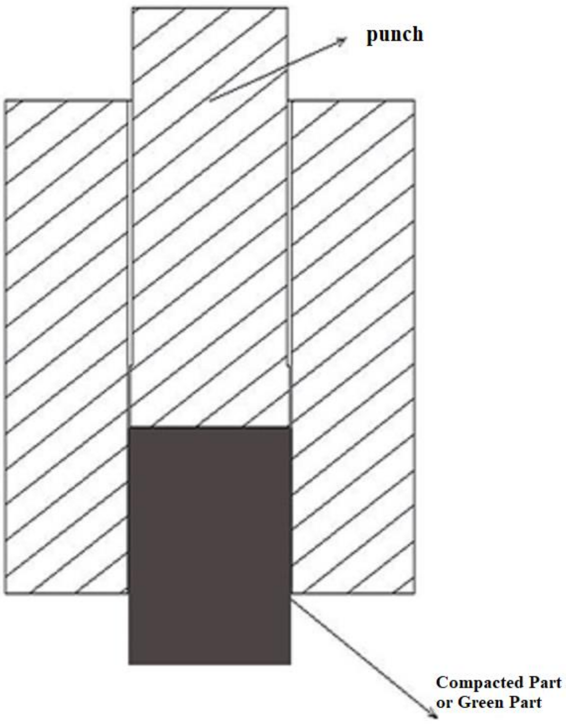

Figure 3: Compaction die with single punch Figure

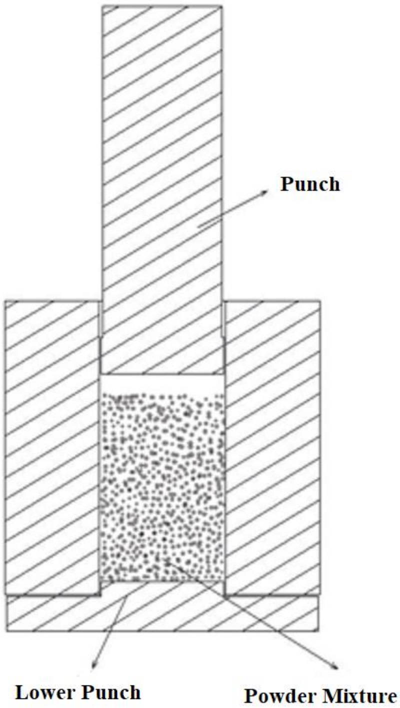

4: Ejection of workpiece from die after compaction

The compaction pressure was 400Mpa at a rate of 10(mm/min) and the ejection pressure of the workpiece from inside the die was 30 Mpa at a rate of 4(mm/min). This was done using a 50-ton press from the Strength of Materials laboratory of the Faculty of Mechanical Engineering at the University of Tabriz (Amsler 50 pzbda401).

Ammonia gas was used as the atmosphere in aluminum sintering. The sintering cycle is shown in Table (3).

Table 3: Sintering cycle of samples

Material	Particle size µm	Raw Density	Atmosphere	Heating rate ($^{\circ}C/_{min}$)	Tempe rature °C	Time min	Dimensional Changes
Aluminu m	52	90	Ammonia (N_2-H_2)	10	600	165	-2

Extrusion of Samples

Extrusion of samples is a post-welding finishing operation primarily aimed at increasing the density of the samples. This increase in density ranges from 90% to 99%. The purpose is to enhance the cohesion of metallurgically powdered samples and ultimately improve their wear resistance.

An extrusion ratio of 6:1 has been considered.

$$A_{\circ}/A_f = 6$$

$$D_{\circ}^2/D_f^2 = 6 \quad , \quad D_{\circ} = 36\ mm$$

Diameter of the sample resulting from extrusion

$$D_f = 14\ mm$$

Length of the sample considering the constant volume of the sample

V = 23072(mm^3) , L = 150mm $\pi/4\,(14)^2 * L =$

Extrusion was carried out at a temperature of 500°C. The mold was heated to the desired temperature using a resistance heating unit, and the components were heated in a furnace controlled by a thermocouple. The mold and dies were made of hot work steel 1.2344 with a hardness of 55 Rockwell, and the surface roughness of the mold was polished to 0.1µm.

A hydraulic press with a capacity of 50 tons was used, with a pressing pressure of 295 MPa or 30 tons in this stage.

Preparation of Wear Test Pins:

The wear test pins were machined from extruded rods with a diameter of 14mm down to a diameter of 8mm and a length of 15mm. The wear surface of the pins was ground to achieve a smoothness between 0.2-0.8µm. Subsequently, they were washed with acetone for 10 minutes and then kept at a temperature of 60°C for 30 minutes to ensure complete drying. An example of one of the pins is shown in Figure (5).

Figure 5: Composite pin with 8 mm diameter

Wear Test:

The wear rate and friction coefficient of composite pins were obtained using the pin-on-disc method. The wear test samples were cylindrical with a diameter of 8mm and a length of 15 *mm*. They were made of an aluminum-based composite. The material of the friction disc was cold work tool steel 1.2080 with a hardness of 62 Rockwell, with dimensions of 100mm in diameter and 10 *mm* in thickness. The surface roughness of the friction disc was prepared by grinding to 0.1 *µm Ra* and then polished.

Vertical forces of 10 *N*, 20 *N*, and 30 *N* were applied to the specimen using a spring, and the tangential force was measured using a load cell to calculate the coefficient of friction. The initial friction coefficient and stable state were determined using the following formula.

$$\mu = F_f / F_p$$

The pin is placed at a diameter of 80mm on the sliding disc. The sliding speeds of the disc are considered to be 0.76 m/s, 1.29 m/s, 5.52 *m/s* and the sliding distance is 5000 meters.

The wear rate was calculated according to formula (1) based on the mass loss per distance traveled (gr / mm^3):

$$W = M/D$$

Where W is the wear rate in terms of weight loss per unit distance traveled (gr/mm^3), M is the weight loss in grams, and D is the distance traveled in meters. The weight loss was measured using a digital balance with a precision of one-thousandth of a gram (2-18). The wear test was conducted under dry conditions at a temperature of 22°C.

Findings:

1. Investigating the Effect of Variations in Sliding Velocity on Wear Rate."

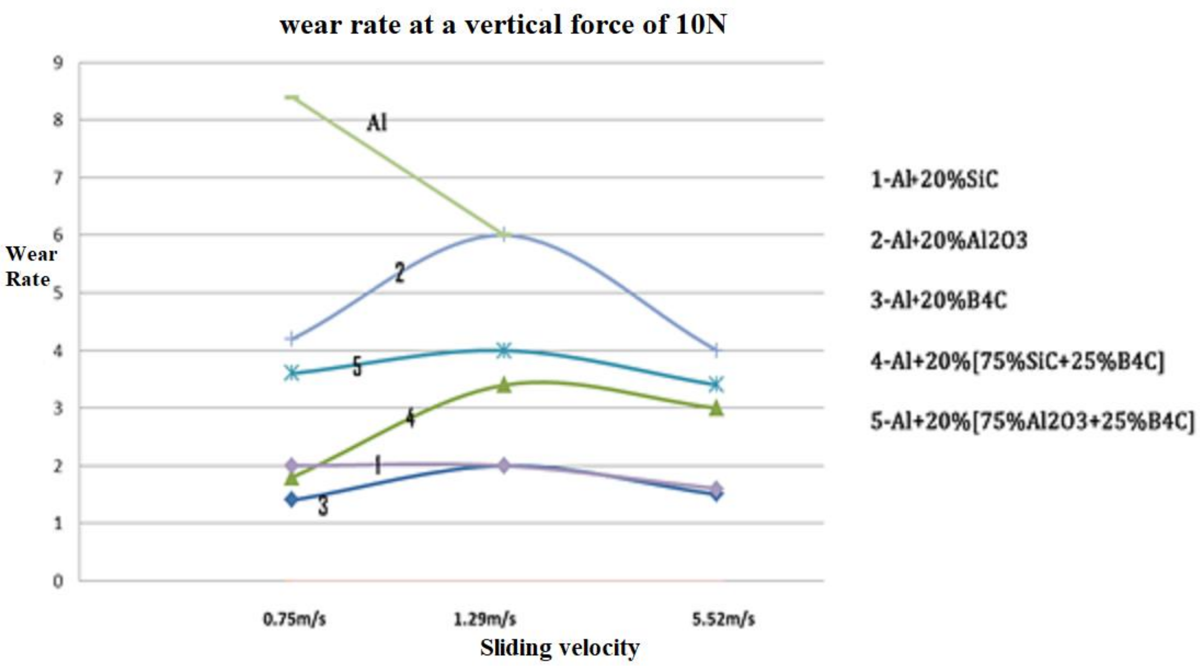

Figure 6: Wear Rates Comparative Graph of Composite Samples

Figure 6 illustrates that, under the test conditions with a constant force of 10N and variable sliding velocities, all composite samples exhibit lower wear rates compared to pure aluminum. In other words, they demonstrate higher wear resistance than pure aluminum. Among the composite samples, the lowest wear rate is associated with the composite containing reinforcing particles B_4C, followed by SiC. The sample labeled as Sample 4, which is a combination of both types of particles, follows in the hierarchy. In these test conditions, samples containing Al_2O_3 particles displayed weaker wear resistance compared to other composite samples. As depicted in the chart, Sample 5 is ranked just after the three previous composites, and then Sample 2, which consists entirely of Al_2O_3 particles. This pattern is consistent across different sliding velocities, with the difference being that at a velocity of 0.75*m/s*, the lowest wear rate is attributed to B_4C. However, at velocities of 1.29*m/s* and 5.52*m/s*, the wear rates of both types of composites with SiC and B_4C particles are almost equal.

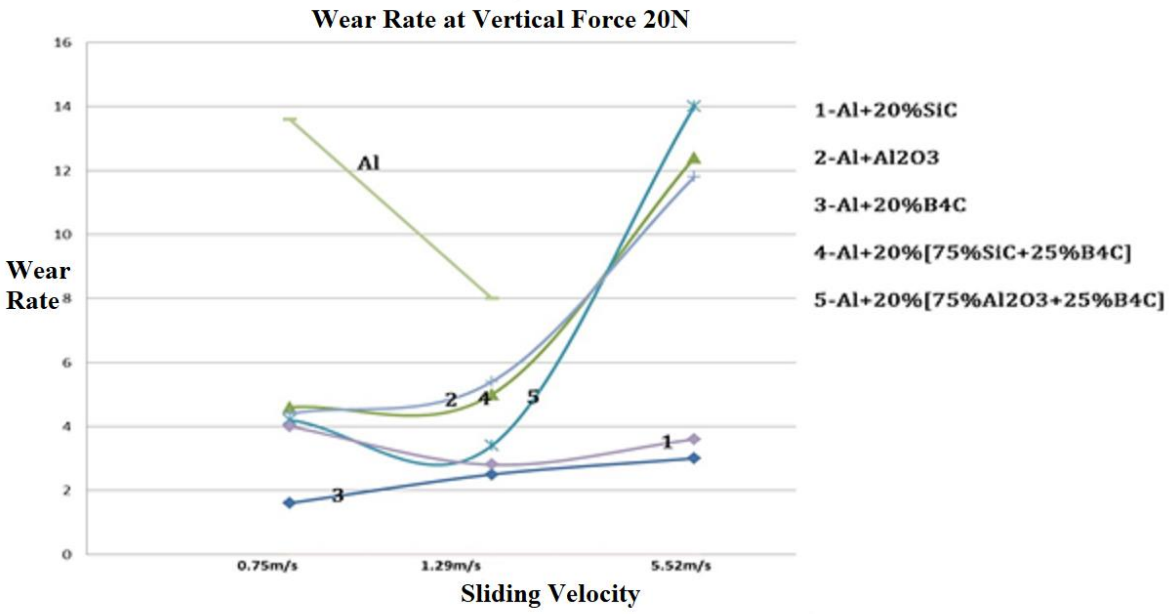

Figure 7: Wear Rates Comparative Graph of Composite Samples

In Figure 7, it is evident that under a constant force of 20 Newtons (20N) and at the speeds where the pure aluminum specimen exhibits wear behavior, the wear rate of composite samples is lower than that of the pure aluminum specimen. Under these test conditions, the composites with reinforcing particles of B_4C and SiC show higher wear resistance compared to other composites. Specifically, at a speed of 0.75 *m/s*, the wear rates are in the following order: Sample 3, followed by Sample 1, while the other samples have nearly equal wear rates. At a speed of 1.29 *m/s*, again, Samples 3 and 1 have the lowest wear rates, followed by the other samples. At a speed of 5.52 *m/s*, Sample 3 exhibits the lowest wear rate, followed by Sample 1, and Sample 2, which contains Al_2O_3 particles, has the highest wear rate. In these test conditions, it is also evident that the effect of B_4C and SiC particles in improving wear resistance is greater than that of Al_2O_3 particles.

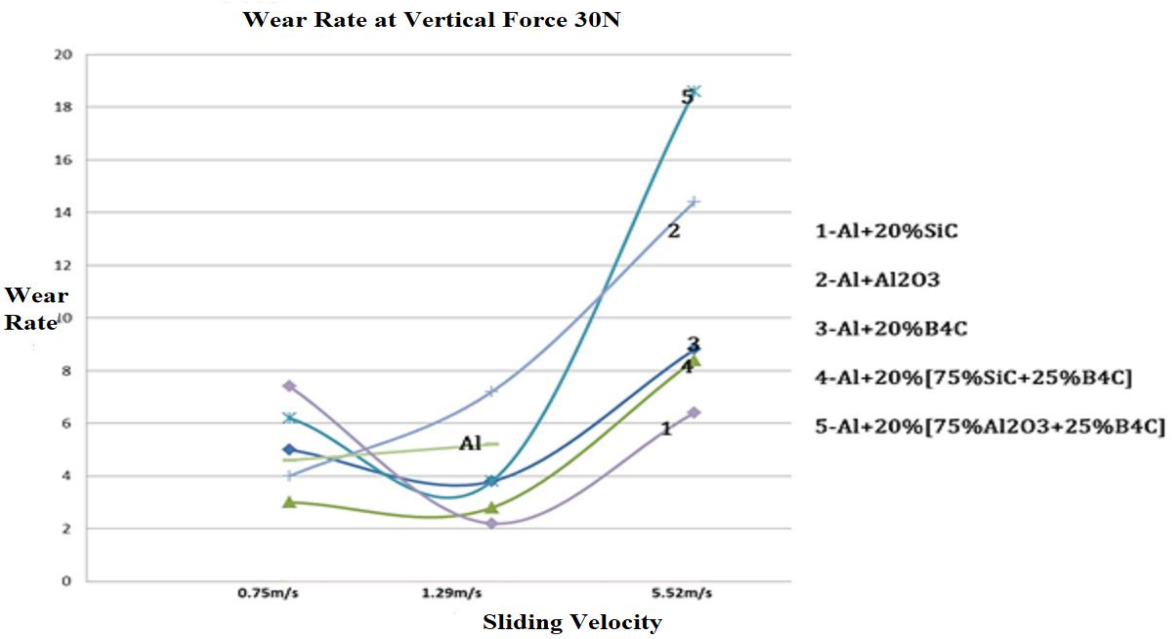

Figure 8: Wear Rates Comparative Graph of Composite Samples

Figure 8 illustrates the wear rates of composite samples under a constant force of 30 Newtons (30N) and variable sliding speeds. In this experiment, it is evident that Samples 1, 4, and 3 exhibit higher wear resistance compared to the other samples. These three samples contain reinforcing particles SiC and B_4C. Additionally, at speeds where pure aluminum exhibited wear behavior, the composite samples generally showed higher wear rates. At a speed of 5.52 *m/s*, the wear rates of the samples significantly increased, reaching up to 18. However, some samples, particularly those containing Al_2O_3 particles, exhibited a sudden increase in wear rates. Samples containing SiC and B_4C particles, on the other hand, remained within a lower range of wear rates.

Therefore, it can be concluded that the samples containing SiC and B_4C particles consistently exhibited better wear resistance than the other samples under all three vertical forces (10N, 20N, and 30N) and at speeds of 0.75 *m/s* and 1.29 *m/s*. At a speed of 5.52 *m/s*, despite the sudden increase in wear rates for some samples, these samples maintained wear rates comparable to those at other speeds. A sliding speed of 1.29 *m/s* can be considered a critical speed because at this speed, the samples exhibited changes in wear behavior. For instance, at a vertical force of 10N, the wear rates of the samples at this speed were the highest compared to other speeds. At vertical forces of 20N and 30N, the wear rates at this speed were the lowest compared to other speeds.

2. Investigating the Effect of Vertical Force Variations on Wear Rate

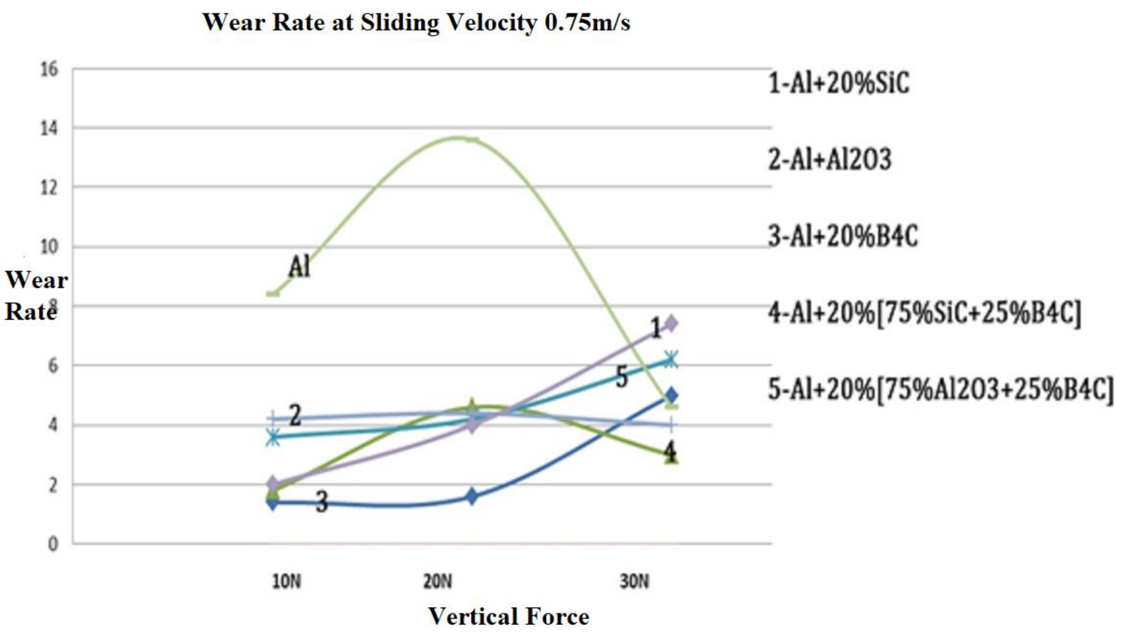

Figure 9: Wear Rates Comparative Graph of Composite Samples

In Figure 9, the wear rates of composite samples relative to each other are shown at a constant speed of 0.75 m/s with varying vertical forces. The wear rates of samples 3, 5, and 1 increase with an increase in vertical force, while samples Al, 4, and 2 initially show an increase in wear rate, but after a vertical force of 20N, their wear rates decrease. A vertical force of 20N appears to be a critical force for samples Al, 4, and 2, where their wear behavior changes. However, overall, the wear rates of composite samples are lower than that of the pure aluminum sample. Among the composite samples, samples 3, 1, and 4 have lower wear rates at vertical forces of 10N and 20N, but at a vertical force of 30N, only sample 4 has a lower wear rate compared to the others. In this experiment, composites containing reinforcing particles such as SiC and B_4C exhibit higher wear resistance compared to other composites.

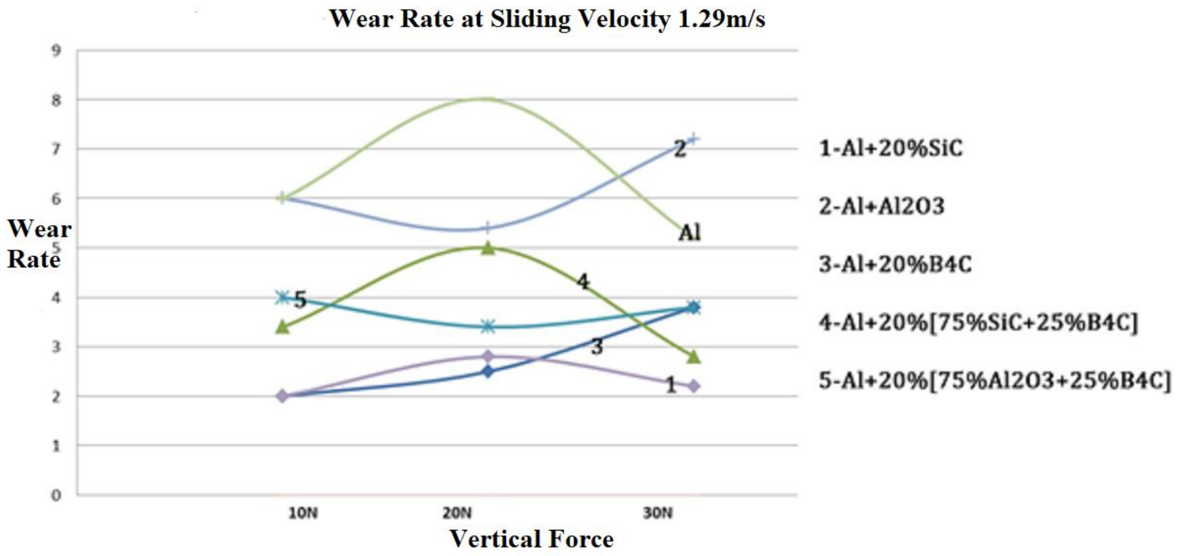

Figure 10: Wear Rates Comparative Graph of Composite Samples

Figure 10 shows the wear rates of composite samples and the pure aluminum sample at a constant speed of 1.29 *m/s* with varying vertical forces. Similar to previous experiments, composites containing SiC and B_4C particles exhibit high wear resistance. Samples 1 and 3 have the lowest wear rates, followed by samples 4, 5, and 2. The wear rates of samples 1, 4, and Al increase initially from 10N to 20N vertical force and then decrease. On the other hand, samples 3, 5, and 2 initially show a decrease in wear rate from 10N to 20N vertical force and then an increase. At the 10N point, samples 3, 1, and 4 have the lowest wear rates, and at the 30N point, these same samples have the lowest wear rates. In this experiment as well, the 20N vertical force appears to be a critical point for wear rates in the composite samples.

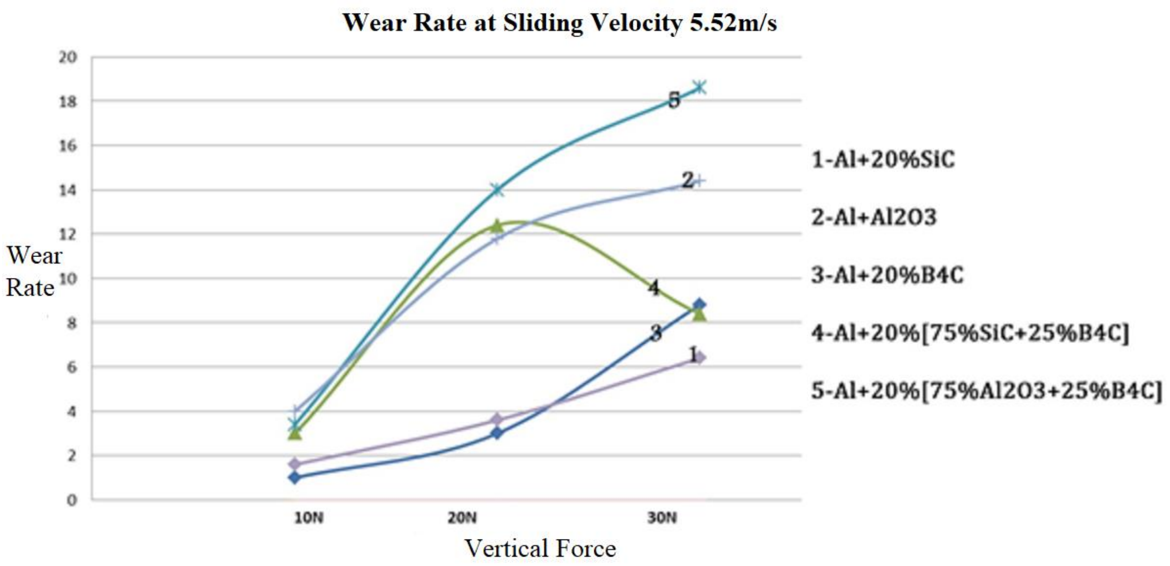

Figure 11: Wear Rates Comparative Graph of Composite Samples

The charts in Figure (11) depict the friction rates of composite samples under constant speed conditions of 5.52 *m/s* and varying vertical forces. In all of these charts, except for sample 4, it is evident that the friction rate increases with an increase in force. Sample 4, on the other hand, shows a reduction in friction rate between forces of 20N and 30N. In this experiment, the pure aluminum sample did not exhibit resistance under these test conditions and could not demonstrate friction behavior; it was destroyed. In this experiment, a force of 20N also represents a critical point for the friction rates of the samples, where the friction behavior of the samples changes. The lowest friction rate in the experiment belongs to samples containing SiC and B_4C particles. In all three forces of 10N, 20N, and 30N, samples 1, 2, and 3 have the lowest friction rates, and the difference in friction rates of these samples compared to the others seems to be more significant.

In general, under constant speed and variable force conditions, samples 5, 1, 2, and 3 gradually exhibit an increase in friction rate with an increase in force from 10N to 30N. However, sample 4 shows a different behavior, as it exhibits an increase in friction rate from 10N to 20N and a decrease in friction rate from 20N to 30N. In summary, a force of 20N represents a critical point for all samples, and if the friction rate does not change at this point, the slope of its decrease or increase will vary.

3. Investigating the Effect of Changes in Sliding Speed on the Friction Coefficient.

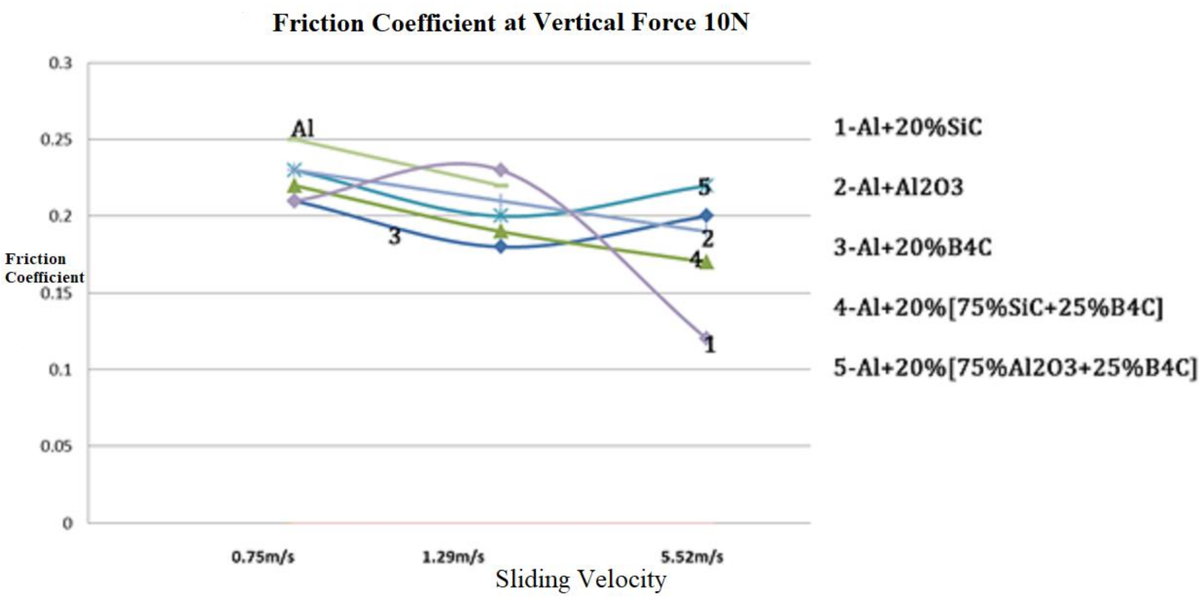

Figure 12: Friction Coefficient Graph of Composite Samples

Figure (12) illustrates the friction coefficients of composite samples under a constant vertical force of 10N with varying sliding speeds. The friction coefficient of all composite samples is lower than that of the pure sample, and this can be attributed to the high frictional resistance of these samples. The lower the coefficient, the lower the friction rate can be. From a sliding speed of 0.75 *m/s* to 1.29 *m/s*, all samples except sample 1 exhibit a decrease in the coefficient, with the sample containing B_4C particles having the lowest coefficient among them. At a speed of 1.29 m/s, the friction behavior of samples 1, 3, and 5 changes, and it becomes reversed up to a speed of 5.52 *m/s*. At this point, the lowest coefficient belongs to the composite with SiC particles. It can be considered that a speed of 1.29 *m/s* is a critical speed for the change in the friction behavior of the samples. In conclusion, the presence of SiC and B_4C particles among the samples has led to a reduction in the friction coefficient.

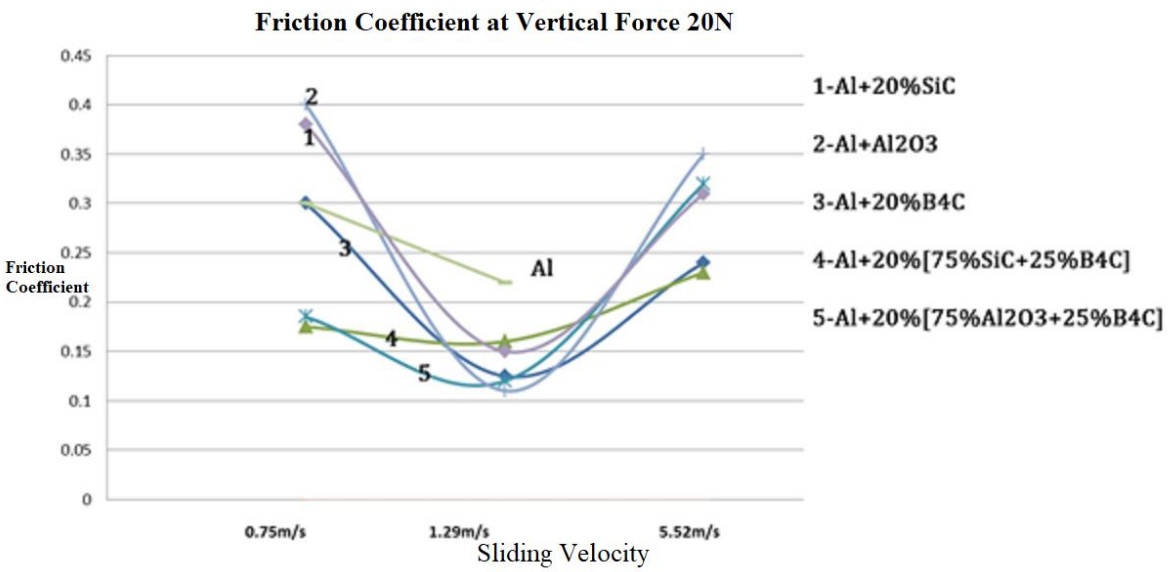

Figure 13: Wear Rate Comparative Graph of Composite Samples

The graphs in Figure 13 depict the friction coefficients of composite samples under a constant force of 10N but with varying sliding velocities. In all samples, as the velocity increases from 0.75 *m/s* to 1.29 *m/s*, the friction coefficient decreases. However, beyond a velocity of 1.29 *m/s*, the coefficient increases for all samples. The friction coefficient for all samples is lower than that of the pure sample, and the critical velocity for this experiment is 1.29m/s. At this velocity, a change in the frictional behavior in the samples is observed, with coefficients varying by up to 0.3. The sample containing SiC and B_4C particles has the lowest coefficient only at the speed of 1.29 *m/s*, while at speeds of 0.75 *m/s* and 5.52 *m/s*, the lowest coefficient is found in sample 4, which consists of a combination of SiC and B_4C particles.

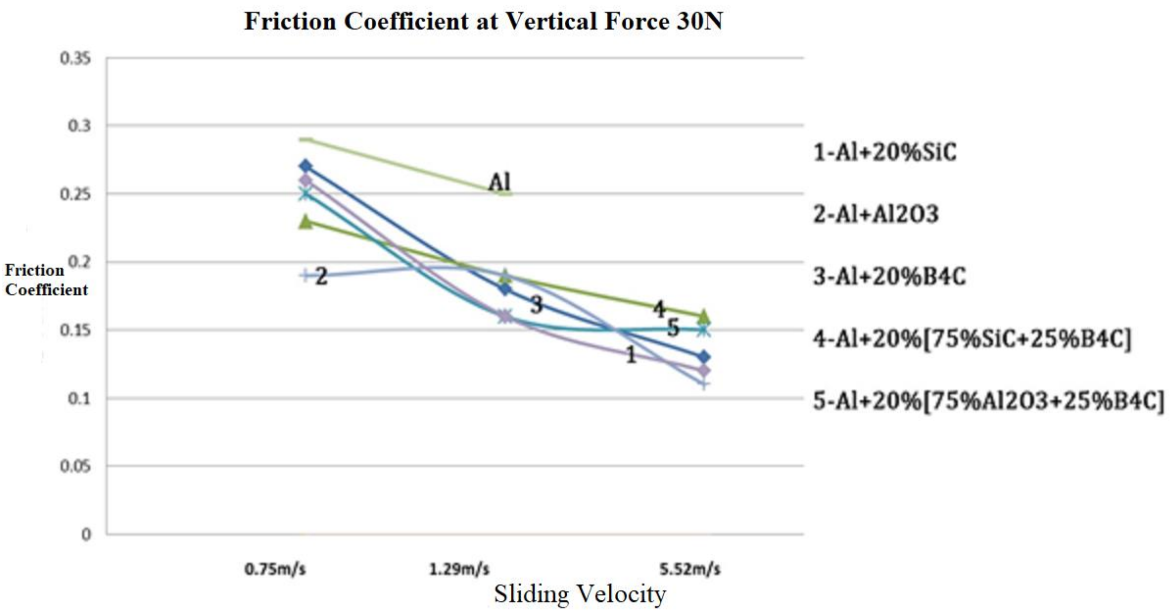

Figure 14: Wear Rate Comparative Graph of Composite Samples

Figure 14 displays the friction coefficients of composite samples under a vertical force of 30N with varying sliding velocities. The dominant trend here is a decrease in the coefficients, meaning that they decrease with an increase in sliding velocity. At higher velocities, the reduction in friction intensity for sample 1 is greater than for all other samples. Once again, in this experiment, the SiC particles contribute to the reduction in friction for sample 1.

Overall, the composite samples, namely Al-20%B_4C, Al-20%Al_2O_3, and Al-20%SiC, exhibited consistent behavior in three different friction experiments with vertical forces of 10N, 20N, and 30N, and variable sliding velocities (0.75m/s, 1.29m/s, 5.52m/s). In all cases, the friction coefficient decreased. Among the samples, the composites Al-20%SiC, Al-20%B_4C, and Al-20%[75%SiC+25%B_4C] had lower friction coefficients and more significant reductions in friction.

4. Investigating the Effect of Vertical Force Variations on Friction Coefficients.

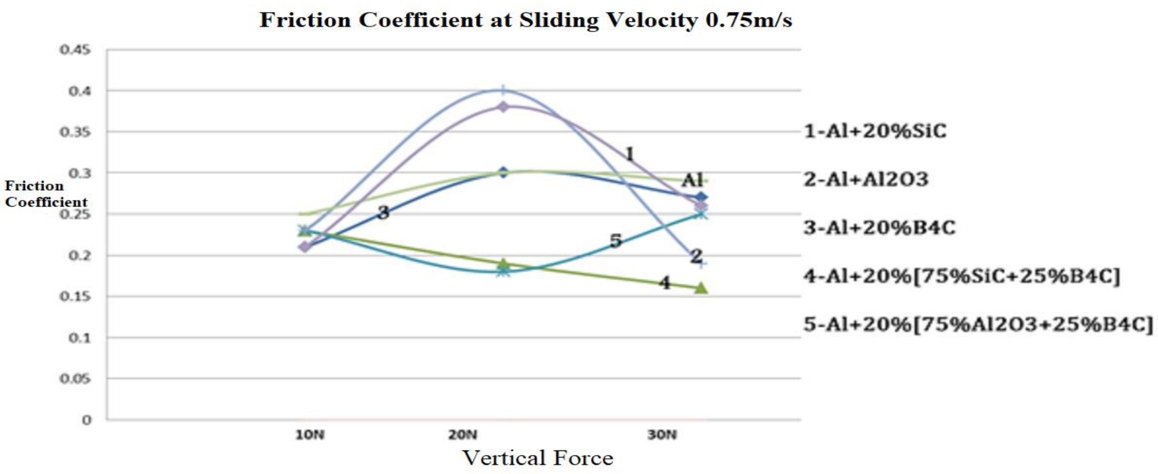

Figure 15: Wear Rate Comparative Graph of Composite Samples

Figure 15 illustrates the friction coefficients of composite samples at a constant velocity of 0.75m/s while varying the vertical force. The graph shows a decrease in the friction coefficient for some samples and an increase for others as the vertical force increases. The lowest coefficient is observed in samples 4 and 5, compared to the other samples and the pure sample. These samples contain SiC and B_4C particles, which could be contributing factors to the reduction in the friction coefficient.

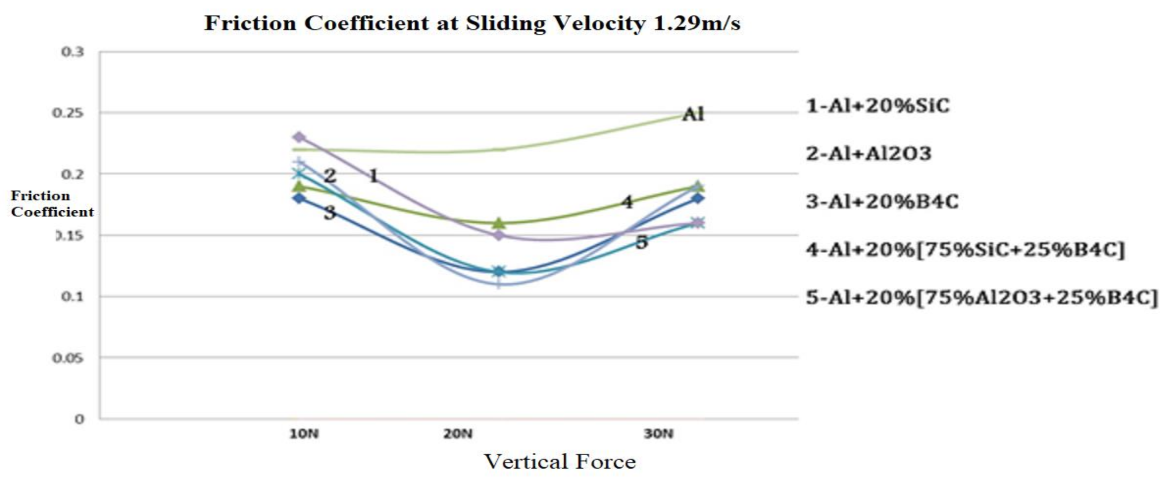

Figure 16: Wear Rate Comparative Graph of Composite Samples

Figure 16 displays the friction coefficients of samples at a constant velocity of 1.29m/s while varying the vertical force. Composite samples have lower friction coefficients compared to the pure sample, primarily due to the presence of ceramic particles in these samples. The behavior of all samples is relatively consistent, such that the friction coefficient decreases from 10N to 20N of force and increases from 20N to 30N with an increase in force. In this experiment as well, sample 3 has the lowest coefficient, while the highest coefficient is associated with the pure aluminum sample.

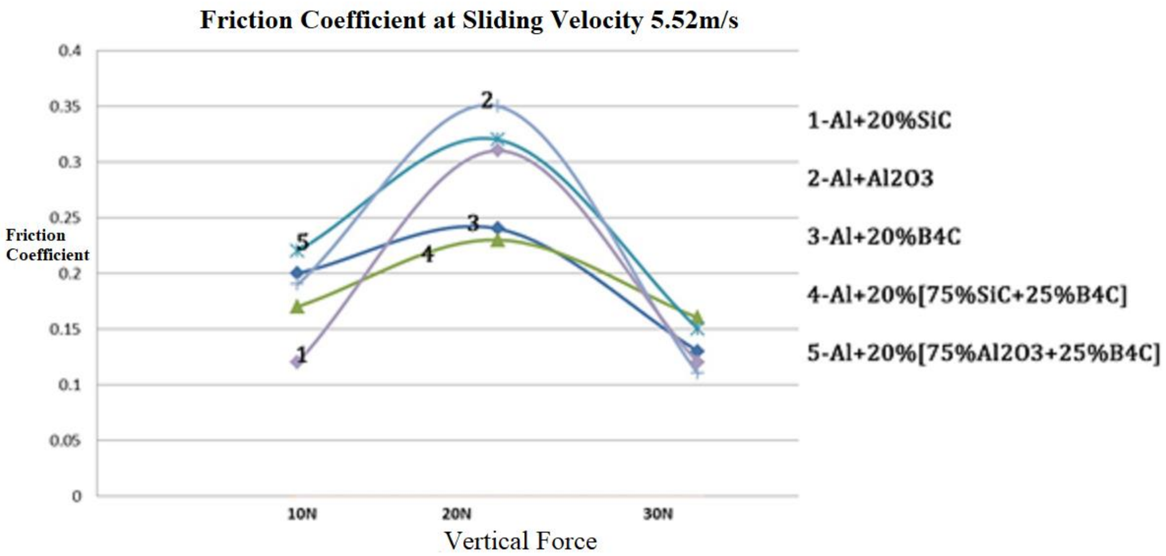

Figure 17: Wear Rate Comparative Graph of Composite Samples

Figure 17 depicts the friction coefficients of composite samples at a constant velocity of 5.52m/s with varying vertical force. Under these test conditions, the pure sample was unable to exhibit any frictional behavior and has been damaged. The frictional behavior of all samples is similar and consistent, where the coefficients initially increase and then decrease with an increase in force. Samples 3 and 4 exhibited the lowest friction coefficients, and it can be attributed to the presence of SiC and B_4C particles, which act as reducing factors in the friction coefficient for these samples.

Conclusion:

In this study, five types of aluminum-based composites, including Al-20%Al_2O_3, Al-20%SiC, Al-20% B_4C, Al-20%[75%SiC+B_4C], and Al-20%[75%Al_2O_3+ B_4C], were fabricated using the powder metallurgy method, and friction tests were conducted. The results of the friction tests for sample 1 showed that the wear rate initially decreases and then increases with an increase in sliding velocity for all three constant forces (10N, 20N, 30N). At constant velocities of 0.75m/s, 1.29m/s, and 5.52m/s, the wear rate increases with an increase in force, except at 1.29m/s, where it decreases as the force increases from 20N to 30N. The friction coefficient also initially increases and then decreases with an increase in velocity at a constant force of 10N, decreases and then increases at 20N, and only decreases at 30N. Additionally, with an increase in force at velocities of 0.75m/s and 5.52m/s, the friction coefficient initially increases and then decreases, while at 1.29m/s, it initially decreases and then increases.

For sample 2, the wear rate increased with an increase in sliding velocity for all three constant forces. However, at 10N force, it decreased between 1.29m/s and 5.52m/s. The friction coefficient decreased with an increase in sliding velocity at constant forces of 10N and 30N, initially decreased and then increased at 20N, and increased with an increase in force at constant velocities. Overall, the friction and wear behavior of the composites exhibited complex patterns dependent on the sliding velocity and applied force.

In sample 3, it is evident that the wear rate increases with an increase in sliding velocity for forces of 20N and 30N, exhibiting an ascending trend. However, at 10N force, the wear rate initially increases and then decreases. Additionally, the wear rate increases with an increase in force at all sliding velocities. The friction coefficient for this sample initially decreases and then, in the case of 10N and 20N forces, increases beyond its initial value with an increase in sliding velocity. At 30N force, it decreases. Moreover, with an increase in force, the friction coefficient increases at sliding velocities of 0.74m/s and 5.52m/s, initially increases and then decreases at 1.29m/s.

Sample 4 shows that the wear rate increases with an increase in sliding velocity for all forces and initially increases and then decreases with an increase in force for all sliding velocities. The friction coefficient for this sample decreases with an increase in sliding velocity at forces of 10N and 30N, increases with an increase in force at sliding velocities of 0.75m/s and 1.29m/s, and exhibits a descending trend at a velocity of 5.52m/s, initially increasing and then decreasing.

In sample 5, the wear rate initially decreases and then increases with an increase in sliding velocity for forces of 20N and 30N, while it initially increases and then decreases at 10N force. Moreover, the wear rate increases with an increase in force at all sliding velocities. The friction coefficient for this sample initially decreases and then increases with an increase in sliding velocity at all forces, and with an increase in force, it initially decreases and then increases at sliding velocities of 0.75m/s and 1.29m/s, while it initially increases and then decreases at 5.52m/s.

References

1. A.S.M.A. Haseeb , K.M. Shorowordi , J.P.Celis , Velocity effects on the wear,friction and tribochemistry of aluminum MMC sliding against phenolic brake pad. Wear 256(2004) 1176-1181 .
2. A.S.M.A Haseeb , K.M. Shorowordi , J.P. Celis , Tribo-surface charact-eristics of Al-B_4C and Al-SiC composites worn under different contact pressure , wear 261 (2006) 634-641.
3. A. Daoud , M.T. Abou El-khair , wear and friction behavior of sand cast brake rotor made of A359-20vol% SiC particle composite sliding against automobile friction material , tribology international 43(2010)544-553.
4. Sun Zhiqiang , Zhang Di , Li Guobin , Evaluation of dry sliding wear behavior of silicon particles reinforced aluminum matrix composites, Materials and Design 26 (2005) 454–458
5. S.Basavarajappa , G.Chandramohan ,et al. Influence of sliding speed on the dry sliding wear behavior and the subsurface deformation on hybrid metal matrix composite , wear 262(2007) 1007-1012.
6. Manoj Singla , Lakhvir Singh , Vikas chawla , Study of wear properties of Al-SiC composite , journal of minerals & materials characterization & engineering , vol. 8, No.10,pp.813-819, 2009.
7. M. Kok , Abrasive wear of Al_2 O_3 particle reinforced 2024 aluminium alloy composite fabricated by vortex method , composite: part A 37 (2006) 457-464 .
8. M.K. Surappa , R.K. Uyyuru , et al. Tribological behavior of Al-Si-SiC_p composite / automobile brake pad system under dry sliding conditions , Tribology international 40 (2007) 365-373 .
9. Shaoyang Zhang , Fuping Wang , Comparison of friction and wear performances of brake material dry sliding against two aluminum matrix composite reinforced with different SiC particles , Journal of material Processing Technology 182(2007)122-127 .
10. Bikramjit Basu , Debdas Roy , et al. Understanding the unlubricated friction and wear behavior of Fe-aluminide reinforced Al-based in-situ metal-matrix composite , composites: Part A37 (2006) 1464-1472 .
11. S.V.Prasad , Aluminum metal matrix composite tailored for antifriction applications , Surface and Coating Technology 54/55(1992) 442-446 .